Journal of Inflammation Research

Dovepress
Taylor & Francis Group

Open Access Full Text Article

ORIGINAL RESEARCH

Development and Validation of an Ileocolonoscopy-Based Nomogram for Predicting Perianal Penetrating Complications in Patients with Crohn's Disease

Siyuan Zhang[1], Jianmin Wang[1], Qing Lin[2], Yuqin Sheng[2], Ming Li[1,3]

[1]Department of Anorectal, The First Affiliated Hospital of Anhui University of Chinese Medicine, Hefei, Anhui, 230031, People's Republic of China; [2]Department of Nursing, Anhui Branch of Shuguang Hospital Affiliated to Shanghai University of Chinese Medicine, Hefei, Anhui, 230031, People's Republic of China; [3]Department of Anorectal, Anhui Branch of Shuguang Hospital Affiliated to Shanghai University of Chinese Medicine, Hefei, Anhui, 230031, People's Republic of China

Correspondence: Ming Li, Department of Anorectal, The First Affiliated Hospital of Anhui University of Chinese Medicine, Hefei, Anhui, 230031, People's Republic of China, Email lmys154@126.com

Background: Perianal penetrating complications (PPC) in Crohn's disease (CD) are inadequately predicted. PPC risk correlates with ileocolonoscopic scores, however, the association between specific ileocolonoscopic features and it remains unclear. This study aimed to identify predictive ileocolonoscopic features and develop a dedicated PPC nomogram, thereby enabling proactive management of high-risk patients. This tool is designed as a prediction model, not a clinical decision-making instrument.

Methods: CD patients from two centers between January 1, 2012 and July 31, 2025 are enrolled: the First Affiliated Hospital of Anhui University of Chinese Medicine (FAHAUTCM, Center 1) and Anhui Branch of Shuguang Hospital Affiliated to Shanghai University of Chinese Medicine (ABSHASUTCM, Center 2). Their demographic and ileocolonoscopic data were collected. Center 1 enrolled patients (n=431) were randomized to training (n=301) and internal validation (n=130) sets at a 7:3 ratio; Center 2 enrolled patients (n=127) served as the external validation set. The Boruta algorithm and Least Absolute Shrinkage and Selection Operator (LASSO) regression identified the most predictive features, which were incorporated into a multivariable logistic regression. Developed model was appraised via Receiver Operating Characteristic (ROC) curves, calibration curves, Decision Curve Analysis (DCA) and nomogram score distribution.

Results: Multivariate logistic regression confirmed five independent predictors: the largest ulcer diameter (OR=1.504, 95% CI=1.095–2.097, P<0.05), ulcer area in rectum (OR=2.900, 95% CI=2.188–3.955, P<0.001), ulcer area in descending colon (OR=1.402, 95% CI=1.005–1.965, P<0.05), nodular lesions (OR=1.976, 95% CI=1.451–2.751, P<0.001), and stenosis (OR=2.544, 95% CI=1.765–3.789, P<0.001). The model achieved AUCs of 0.857 (internal validation) and 0.847 (external validation), with favorable calibration (P=0.240 and 0.498 for Hosmer–Lemeshow tests, respectively). DCA and nomogram score distribution further verified the model's clinical utility.

Conclusion: We identified several ileocolonoscopic predictors and developed a nomogram which showed good predictive accuracy. This nomogram overcomes the limitations of common scoring systems, which assign equal weight to all intestinal segmental lesions. It enables rapid clinical risk stratification without complex calculations and helps clinicians consider personalized surveillance.

Keywords: Crohn's disease, ileocolonoscopy, prediction nomogram model, complications

Introduction

Crohn's disease (CD) is a chronic gastrointestinal inflammatory disorder. Its perianal penetrating complications (PPC)—including anal fistula and perianal abscess—are debilitating that manifest as swelling, pain, and discharge of pus, feces or blood. More worryingly, patients with PPC have a threefold risk of anorectal malignancy and higher mortality compared with the general population.[1,2] Surveys indicated the incidence of PPC among CD patients varies from 39.2% to 56.1%.[3]

https://doi.org/10.2147/JIR.S594754
Received: 8 January 2026
Accepted: 13 March 2026
Published: 20 March 2026

However, PPC has an insidious onset, with clinicians usually conducting examinations and adjusting treatment regimens only after overt symptoms emerge; this reveals substantial gaps in PPC monitoring and management, consistent with concerns highlighted in the recently updated European Crohn's and Colitis Organization (ECCO) guidelines.[4]

Colonic and rectal involvement is a well-established risk factor for PPC in CD, while isolated ileal disease exerts a protective effect; this anatomical association is the core rationale for our study to identify segment-specific ileocolonoscopic features for PPC prediction.[5] Existing PPC prediction models for CD are mostly based on serum biomarkers[6] or imaging indicators,[7] with few models focusing on Ileocolonoscopic features, which are closely linked to PPC pathogenesis.

Ileocolonoscopy serves as the first-line approach for CD diagnosis and The Simple Endoscopic Score for CD (SES-CD) and CD Endoscopic Index of Severity (CDEIS) are critical for evaluation of prognosis. Studies confirmed that reduced scores correlate strongly with better long-term outcomes, including lower risks of perianal lesions.[8,9] Nevertheless, these scoring systems have clinical limitations: scores require segmental calculation with equal weighting assigned to each intestinal segment, even though involved intestinal sites are closely correlated with PPC development.[10] Most importantly, it remains unclear which ileocolonoscopic features—whether included in these systems or not—are predictive risk factors for PPC.

PPC is a key phenotype of transmural penetrating CD, along with upper gastrointestinal penetrating lesions, entero-enteric fistulas, and postoperative anastomotic complications. These entities share chronic transmural inflammation as a common pathological basis, and mucosal lesions seen on ileocolonoscopy serve as direct biomarkers of the inflammatory burden driving penetrating disease. However, few studies have explored the value of ileocolonoscopic mucosal features in predicting PPC.

Thus, we incorporated demographic and ileocolonoscopic characteristics into the study and constructed a straightforward nomogram to predict PPC of CD patients. It also exhibited excellent performance in both internal and external validation. Ileocolonoscopy is only a component of comprehensive PPC risk stratification. Complementary modalities including cross-sectional imaging, nutritional status and systemic inflammatory markers also contribute to risk assessment. Our model aims to complement rather than replace them. Our study highlights the novel value of ileocolonoscopy in early identification and intervention of CD complications.

Materials and Methods

This study is in adherence to the TRIPOD (Transparent Reporting of a multivariable prediction model for Individual Prognosis or Diagnosis).[11] The completed checklist is provided as Supplementary Figure - TRIPOD Checklist.

Patient Population

Our study was designed as a two-center retrospective study. Approved by the Institutional Review Board, we enrolled patients diagnosed with CD at the First Affiliated Hospital of Anhui University of Chinese Medicine (FAHAUTCM, Center 1) and Anhui Branch of Shuguang Hospital Affiliated to Shanghai University of Chinese Medicine (ABSHASUTCM, Center 2) between January 1, 2012, and July 31, 2025, with patient informed consent requirements waived. The diagnosis of CD was following the ECCO guidelines.[4]

Inclusion criteria: (1) Complete demographic and ileocolonoscopic data within 7 days of baseline; (2) No ileocolonoscopic treatment (including endoscopic balloon dilation, endoscopic stricturotomy, endoscopic fistula treatment, endoscopic abscess drainage, and endoscopic mucosal or lesion management, etc.) at baseline; (3) No concomitant Montreal p phenotype (perianal fistulas and abscesses); (4) A minimum 3-month follow-up. Exclusion criteria: (1) Age of onset < 14 years; (2) Suboptimal ileocolonoscopic imaging quality; (3) Fewer than 4 intestinal segments available for valid exploration (the segments to be examined include the terminal ileum, ascending colon, transverse colon, descending colon, and rectum, with an insertion depth of at least 10 cm defined as valid exploration of the corresponding intestinal segment)[12] due to various causes (including impassable stenosis, intestinal resection, etc).; (4) Comorbidity with gastrointestinal malignancy, infectious diseases, or other intestinal inflammatory disorders (ulcerative colitis, intestinal tuberculosis, intestinal Behçet's disease, etc).

Sample size estimation was performed following the approach outlined by Riley et al[13] The prevalence of PPC among Asian CD patients ranges from 9.3%[14] to 61%.[15] A total of 21 candidate parameters were included with a shrinkage

factor of 0.9 and an expected Cox-Snell R^2 of 0.25. The calculated sample size was 793 cases when the prevalence was set at 9.3%, and 646 cases when the prevalence was set at 61%.

Candidate characteristics including demographic and ileocolonoscopic characteristics were selected based on a synthesis of expertise and literature. The demographic characteristics included gender, age, drinking history, smoking history, disease duration (time from symptom onset to CD diagnosis) and body mass index (BMI). The ileocolonoscopic characteristics documented included the largest ulcer diameter, deep ulcer, edema and hyperemia area, ulcer area, nodular lesions, stenosis and intestinal fistula. Patients enrolled from Center 1 were randomly distributed to a training set and an internal validation set at a 7:3 ratio. Patients' recruitment flow and grouping strategy are shown in Figure 1.

Baseline and Endpoint

CD diagnosis was defined as baseline, and PPC occurrence as the endpoint. Patients were censored at loss to follow-up or study end (November 30, 2025). Only those with follow-up >3 months were included using their last observed status; the others were excluded for not meeting the minimum follow-up requirement. PPC diagnosis required confirmation by clinical manifestations, digital rectal examination, and imaging.[4]

Ileocolonoscopic Examination

Bowel preparation: Following the Chinese Guidelines for Bowel Preparation,[16] patients were prescribed a low-residue diet for 72 hours pre-examination, with only a clear liquid diet permitted on the day prior. 1L of polyethylene glycol and electrolyte oral solution (PEG-ELS) was administered orally within 1 hour on the eve of the examination. Patients fasted on the examination day and ingested the remaining 3 L of PEG-ELS 4–6 hours pre-procedure, at 250 mL intervals every 15 minutes. The final 1 L of PEG-ELS was mixed with 20 mL of dimethicone before administration.

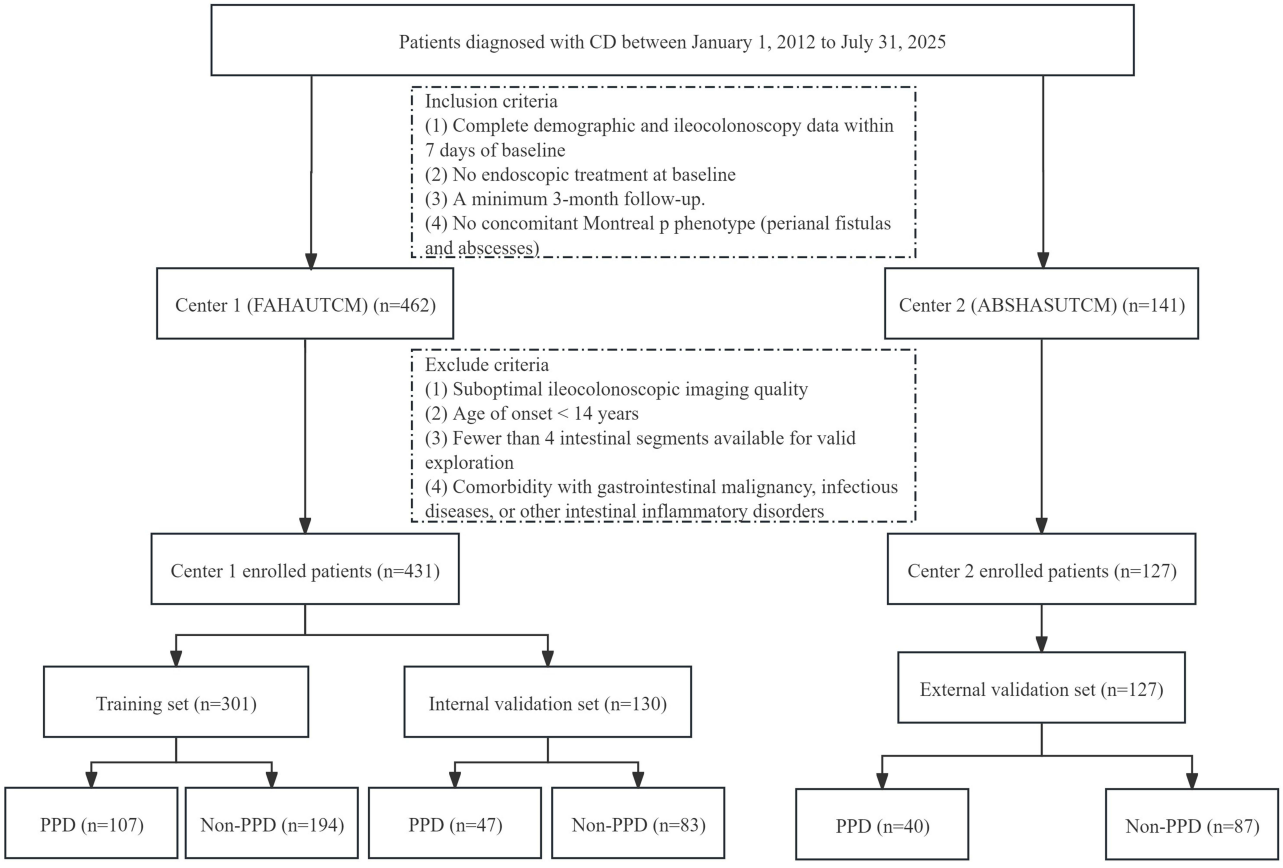

Figure 1 Flowchart of patient recruitment and grouping.

https://doi.org/10.2147/JIR.S594754

Personnel allocation and blinding method: Ileocolonoscopic examinations at 2 centers were performed by 3 senior endoscopists from Center 1 (≥ 100 CD case experience each): two conducted and documented examinations, the third resolved discrepancies. Crucially, they were blinded to patients' disease status and other examination findings, with no involvement in later management.

Examination and documentation: Patients assumed a left lateral decubitus position with flexed knees, followed by digital rectal examination to detect strictures, anal fissures, hemorrhoids, and other anorectal anomalies. They were instructed to breathe orally and relax the anal sphincter for scope insertion. The endoscopist gently inserted the scope into the anus, advanced it to the ileocecal valve, and tried to intubate the terminal ileum as deeply as possible. Systematic imaging and recording of all relevant parameters were completed during the procedure.

Management of adverse reactions: The examination was stopped at once in case of patients' intolerance or adverse events.

Statistical Analysis

Missing data were assessed for all candidate variables prior to model construction. Variables with missing data >20% were excluded. For missing values of 5–20%, multiple imputation was performed under the missing-at-random assumption. Five imputed datasets were generated using chained equations including clinical and outcome variables. Pooled estimates were obtained via Rubin's rules, and complete-case analysis was used for sensitivity analysis. For missing data <5%, median imputation was used for non-normally distributed continuous variables and mode imputation for ordinal categorical variables.

Continuous data with normal distribution were presented as mean ± standard deviation and compared via independent samples *t*-test; non-normally distributed continuous data were expressed as Median (IQR) and compared using Mann–Whitney *U*-test. Categorical data were summarized as n (%) and compared with chi-square test. All continuous variables were standardized (mean = 0, SD = 1) before analysis. Least Absolute Shrinkage and Selection Operator (LASSO) and Boruta algorithm were then used to address high-dimensional multicollinearity and identify high-predictive features.

The events per variable (EPV) ratio was 19.4 (194 incident PPC events and 5 candidate predictors), well above the recommended minimum threshold of 10 for logistic regression-based clinical prediction models,[17] thus effectively reducing overfitting risk. Further measures to guard against overfitting included 10-fold cross-validation during LASSO feature selection, together with independent internal and external validation to assess model generalizability.

Multivariable logistic regression was prespecified as the primary modeling approach, consistent with our objective to develop a clinically interpretable nomogram for individualized absolute PPC risk prediction at initial CD diagnosis. As the gold-standard method for nomogram development, it provides direct absolute risk estimates for bedside risk stratification, with excellent interpretability for the binary PPC endpoint and low overfitting risk.

Before formal modeling, key assumptions of multivariable logistic regression were thoroughly checked. The linearity assumption in the logit for all continuous predictors was verified using Box–Tidwell tests. No multicollinearity was detected among candidate predictors, as all variance inflation factors (VIF) values were less than 2. Detailed processing and coding rules for variables are provided in Supplementary File - Variable Coding Rules and Handling Methods.

Finally, multivariate logistic regression was employed to adjust for confounding factors and screen stable, significant predictors for model construction. Receiver Operating Characteristic (ROC) curves were constructed to evaluate the model's discriminative ability, with the Area Under the ROC Curve (AUC) and 95% confidence intervals (CIs) reported. Calibration curves were plotted to assess the consistency between predicted and observed PPC risks, with calibration slopes calculated to quantify goodness of fit; the Hosmer–Lemeshow test was additionally performed for calibration assessment. Decision Curve Analysis (DCA) and nomogram score distribution analysis were used to validate the model's clinical utility and diagnostic performance. A two-tailed *t*-test was used, with $P < 0.05$ considered statistically significant. Statistical analyses were performed using SPSS 24 and R software (http://www.R-project.org).

Result

Baseline Characteristics

431 patients were enrolled in Center 1. No variables had a missing rate exceeding 20%, so no variables were excluded from the analysis. Only two variables had missing data: edema and hyperemia area in the terminal ileum, and ulcer area in the terminal ileum, with an overall missing rate of 2.6% in the Center 1 cohort and 2.4% in the Center 2 cohort (all <5%). Table 1 presents the demographic and ileocolonoscopic characteristics of enrolled patients in the two centers, and Table 2 shows those of patients in the two subgroups of Center 1. Besides, baseline medications and Montreal

Table 1 Comparison of Demographic and Ileocolonoscopy Characteristics Between Enrolled Patients in Center 1 and Center 2

Characteristics	Total (n = 558)	Center 1 (n = 431)	Center 2 (n = 127)	P-value
PPC, n (%)				0.439
No	364 (65)	277 (64)	87 (69)	
Yes	194 (35)	154 (36)	40 (31)	
Age, years, median (IQR)	31 (25, 35)	31 (25, 35)	31 (24, 34.5)	0.335
Gender, n (%)				0.691
Female	146 (26)	115 (27)	31 (24)	
Male	412 (74)	316 (73)	96 (76)	
BMI, kg/m^2, median (IQR)	20.34 (19.34, 21.73)	20.42 (19.39, 21.73)	20.15 (19.16, 21.54)	0.192
Disease duration, months, median (IQR)	10 (5, 14)	10 (5, 15)	10 (5, 14)	0.425
Smoking history, n (%)				0.333
No	387 (69)	294 (68)	93 (73)	
Yes	171 (31)	137 (32)	34 (27)	
Drinking history, n (%)				0.093
No	372 (67)	279 (65)	93 (73)	
Yes	186 (33)	152 (35)	34 (27)	
Ulcer area				
Ulcer area in rectum, n (%)				0.722
0	195 (35)	155 (36)	40 (31)	
<10%	99 (18)	76 (18)	23 (18)	
10–29%	87 (16)	68 (16)	19 (15)	
≥30%	177 (32)	132 (31)	45 (35)	
Ulcer area in descending colon, n (%)				0.363
0	159 (28)	125 (29)	34 (27)	
<10%	155 (28)	120 (28)	35 (28)	
10–29%	141 (25)	102 (24)	39 (31)	
≥30%	103 (18)	84 (19)	19 (15)	
Ulcer area in transverse colon, n (%)				0.949
0	164 (29)	124 (29)	40 (31)	
<10%	101 (18)	79 (18)	22 (17)	
10–29%	167 (30)	130 (30)	37 (29)	
≥30%	126 (23)	98 (23)	28 (22)	
Ulcer area in ascending colon, n (%)				0.43
0	202 (36)	150 (35)	52 (41)	
<10%	135 (24)	106 (25)	29 (23)	
10–29%	189 (34)	152 (35)	37 (29)	
≥30%	32 (6)	23 (5)	9 (7)	
Ulcer area in terminal ileum, n (%)				0.382
0	266 (48)	199 (46)	67 (53)	
<10%	223 (40)	174 (40)	49 (39)	
10–29%	56 (10)	46 (11)	10 (8)	
≥30%	13 (2)	12 (3)	1 (1)	

(*Continued*)

https://doi.org/10.2147/JIR.S594754

Table 1 (Continued).

Characteristics	Total (n = 558)	Center 1 (n = 431)	Center 2 (n = 127)	P-value
The largest ulcer diameter, cm, median (IQR)	2.5 (1.8, 3.2)	2.5 (1.8, 3.2)	2.6 (1.8, 3.2)	0.457
Deep ulcer, n (%)				0.15
No	221 (40)	162 (38)	59 (46)	
Single	174 (31)	136 (32)	38 (30)	
Multiple	163 (29)	133 (31)	30 (24)	
Edema and hyperemia area				
Edema and hyperemia area in rectum, n (%)				0.404
0	191 (34)	141 (33)	50 (39)	
<50%	159 (28)	122 (28)	37 (29)	
50–69%	124 (22)	99 (23)	25 (20)	
≥70%	84 (15)	69 (16)	15 (12)	
Edema and hyperemia area in descending colon, n (%)				0.487
0	236 (42)	178 (41)	58 (46)	
<50%	135 (24)	109 (25)	26 (20)	
50–69%	104 (19)	83 (19)	21 (17)	
≥70%	83 (15)	61 (14)	22 (17)	
Edema and hyperemia area in transverse colon, n (%)				0.343
0	172 (31)	127 (29)	45 (35)	
<50%	187 (34)	142 (33)	45 (35)	
50–69%	120 (22)	97 (23)	23 (18)	
≥70%	79 (14)	65 (15)	14 (11)	
Edema and hyperemia area in ascending colon, n (%)				0.214
0	159 (28)	123 (29)	36 (28)	
<50%	122 (22)	95 (22)	27 (21)	
50–69%	140 (25)	115 (27)	25 (20)	
≥70%	137 (25)	98 (23)	39 (31)	
Edema and hyperemia area in terminal ileum, n (%)				0.086
0	206 (37)	150 (35)	56 (44)	
<50%	232 (42)	180 (42)	52 (41)	
50–69%	55 (10)	44 (10)	11 (9)	
≥70%	65 (12)	57 (13)	8 (6)	
Nodular lesions, n (%)				0.967
No	328 (59)	253 (59)	75 (59)	
Single	106 (19)	81 (19)	25 (20)	
Scattered	73 (13)	58 (13)	15 (12)	
Cobblestone appearance	51 (9)	39 (9)	12 (9)	
Stenosis, n (%)				0.938
No	169 (30)	133 (31)	36 (28)	
Single	182 (33)	140 (32)	42 (33)	
Multiple	172 (31)	132 (31)	40 (31)	
Cannot pass	35 (6)	26 (6)	9 (7)	
Intestinal fistula, n (%)				0.468
No	548 (98)	422 (98)	126 (99)	
Yes	10 (2)	9 (2)	1 (1)	

Notes: Data following a normal distribution are shown as the mean ± SD, while those not normally distributed are depicted as median (IQR) and categorical variables are displayed as count (%).

Abbreviations: PPC, perianal penetrating complications; BMI, Body Mass Index; IQR, Interquartile Range.

Table 2 Comparison of Demographic and Ileocolonoscopy Characteristics Between Patients in Training Set and Internal Validation Set

Characteristics	Total (n = 431)	Internal Validation set (n = 130)	Training Set (n = 301)	P-value
PPC, n (%)				0.991
No	277 (64)	83 (64)	194 (64)	
Yes	154 (36)	47 (36)	107 (36)	
Age, years, median (IQR)	31 (25, 35)	31 (26, 35)	31 (25, 36)	0.656
Gender, n (%)				0.778
Female	115 (27)	33 (25)	82 (27)	
Male	316 (73)	97 (75)	219 (73)	
BMI, kg/m^2 (mean±SD)	20.53 ± 1.65	20.63 ± 1.67	20.49 ± 1.65	0.444
Disease duration, months, median (IQR)	10 (5, 15)	10 (5, 14)	11 (5, 15)	0.8
Smoking history, n (%)				0.474
No	294 (68)	85 (65)	209 (69)	
Yes	137 (32)	45 (35)	92 (31)	
Drinking history, n (%)				0.307
No	279 (65)	79 (61)	200 (66)	
Yes	152 (35)	51 (39)	101 (34)	
Ulcer area in rectum, n (%)				0.904
0	155 (36)	47 (36)	108 (36)	
<10%	76 (18)	24 (18)	52 (17)	
10–29%	68 (16)	18 (14)	50 (17)	
≥30%	132 (31)	41 (32)	91 (30)	
Ulcer area in descending colon, n (%)				0.235
0	125 (29)	44 (34)	81 (27)	
<10%	120 (28)	28 (22)	92 (31)	
10–29%	102 (24)	32 (25)	70 (23)	
≥30%	84 (19)	26 (20)	58 (19)	
Ulcer area in transverse colon, n (%)				0.184
0	124 (29)	37 (28)	87 (29)	
<10%	79 (18)	19 (15)	60 (20)	
10–29%	130 (30)	48 (37)	82 (27)	
≥30%	98 (23)	26 (20)	72 (24)	
Ulcer area in ascending colon, n (%)				0.421
0	150 (35)	47 (36)	103 (34)	
<10%	106 (25)	29 (22)	77 (26)	
10–29%	152 (35)	50 (38)	102 (34)	
≥30%	23 (5)	4 (3)	19 (6)	
Ulcer area in terminal ileum, n (%)				0.41
0	199 (46)	62 (48)	137 (46)	
<10%	174 (40)	48 (37)	126 (42)	
10–29%	46 (11)	14 (11)	32 (11)	
≥30%	12 (3)	6 (5)	6 (2)	
The largest ulcer diameter, cm, median (IQR)	2.5 (1.8, 3.2)	2.45 (1.8, 3)	2.5 (1.8, 3.2)	0.42
Deep ulcer, n (%)				0.887
No	162 (38)	47 (36)	115 (38)	
Single	136 (32)	43 (33)	93 (31)	
Multiple	133 (31)	40 (31)	93 (31)	
Edema and hyperemia area in rectum, n (%)				0.766
0	141 (33)	41 (32)	100 (33)	
<50%	122 (28)	34 (26)	88 (29)	
50–69%	99 (23)	31 (24)	68 (23)	
≥70%	69 (16)	24 (18)	45 (15)	

(*Continued*)

https://doi.org/10.2147/JIR.S594754

Table 2 (Continued).

Characteristics	Total (n = 431)	Internal Validation set (n = 130)	Training Set (n = 301)	P-value
Edema and hyperemia area in descending colon, n (%)				0.296
0	178 (41)	60 (46)	118 (39)	
<50%	109 (25)	35 (27)	74 (25)	
50–69%	83 (19)	21 (16)	62 (21)	
≥70%	61 (14)	14 (11)	47 (16)	
Edema and hyperemia area in transverse colon, n (%)				0.427
0	127 (29)	43 (33)	84 (28)	
<50%	142 (33)	36 (28)	106 (35)	
50–69%	97 (23)	32 (25)	65 (22)	
≥70%	65 (15)	19 (15)	46 (15)	
Edema and hyperemia area in ascending colon, n (%)				0.226
0	123 (29)	39 (30)	84 (28)	
<50%	95 (22)	35 (27)	60 (20)	
50–69%	115 (27)	33 (25)	82 (27)	
≥70%	98 (23)	23 (18)	75 (25)	
Edema and hyperemia area in terminal ileum, n (%)				0.764
0	150 (35)	42 (32)	108 (36)	
<50%	180 (42)	55 (42)	125 (42)	
50–69%	44 (10)	16 (12)	28 (9)	
≥70%	57 (13)	17 (13)	40 (13)	
Nodular lesions, n (%)				0.289
No	253 (59)	76 (58)	177 (59)	
Single	81 (19)	22 (17)	59 (20)	
Scattered	58 (13)	23 (18)	35 (12)	
Cobblestone appearance	39 (9)	9 (7)	30 (10)	
Stenosis, n (%)				0.259
No	133 (31)	45 (35)	88 (29)	
Single	140 (32)	46 (35)	94 (31)	
Multiple	132 (31)	34 (26)	98 (33)	
Cannot pass	26 (6)	5 (4)	21 (7)	
Intestinal fistula, n (%)				0.73
No	422 (98)	128 (98)	294 (98)	
Yes	9 (2)	2 (2)	7 (2)	

Notes: Data following a normal distribution are shown as the mean ± SD, while those not normally distributed are depicted as median (IQR) and categorical variables are displayed as count (%).

Abbreviations: PPC, perianal penetrating complications; BMI, Body Mass Index; SD, Standard Deviation; IQR, Interquartile Rang.

classification of disease location and behavior were reported in Supplementary File - Supplementary Table. Figure 2 displays representative ileocolonoscopic images of characteristics.

Feature Selection

Boruta algorithm and LASSO regression were used for feature screening. Boruta identified 7 noteworthy features from all variables (Figure 3A). LASSO regression with 10-fold cross-validation determined the optimal model with 8 variables (Figure 3B and C). The intersection of them was used to identify features for multivariate logistic regression: the largest ulcer diameter, ulcer area in rectum, ulcer area in descending colon, nodular lesions, stenosis.

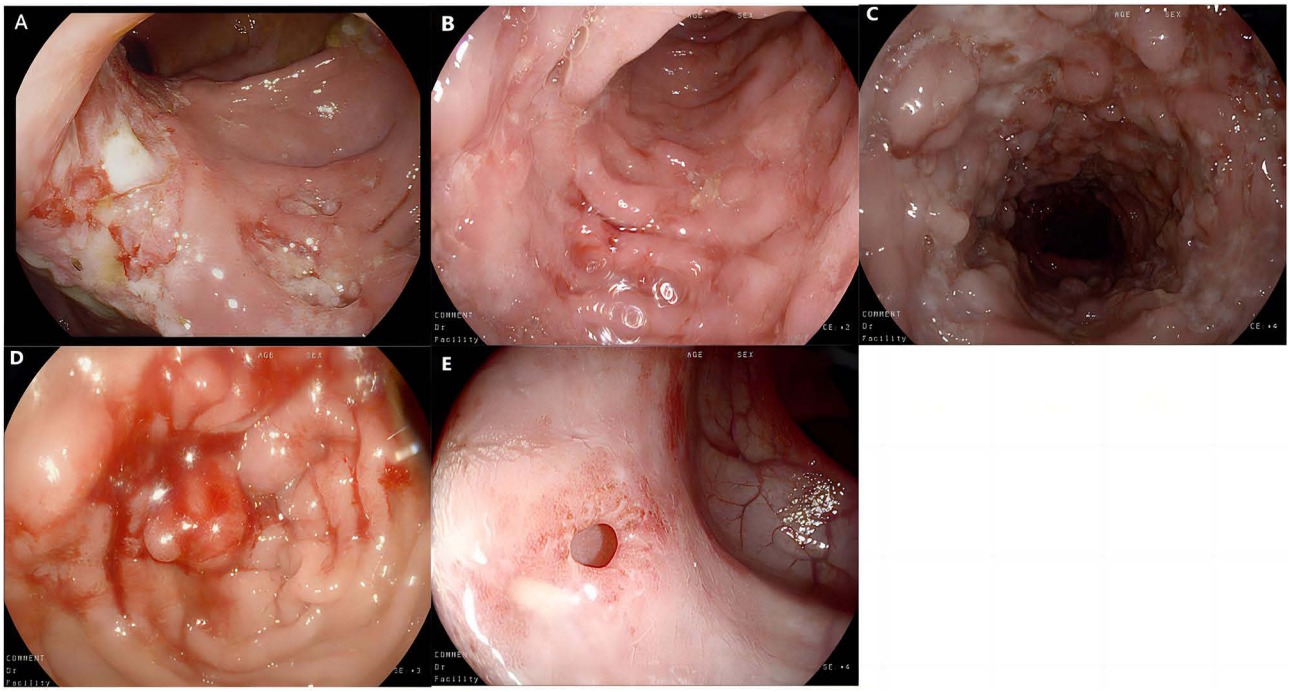

Figure 2 Representative ileocolonoscopic images of typical characteristics. (**A**) Deep and large ulcer. (**B**) Mucosal edema and hyperemia. (**C**) Nodular lesions (cobblestone sign). (**D**) Stenosis (cannot pass). (**E**) Intestinal fistula.

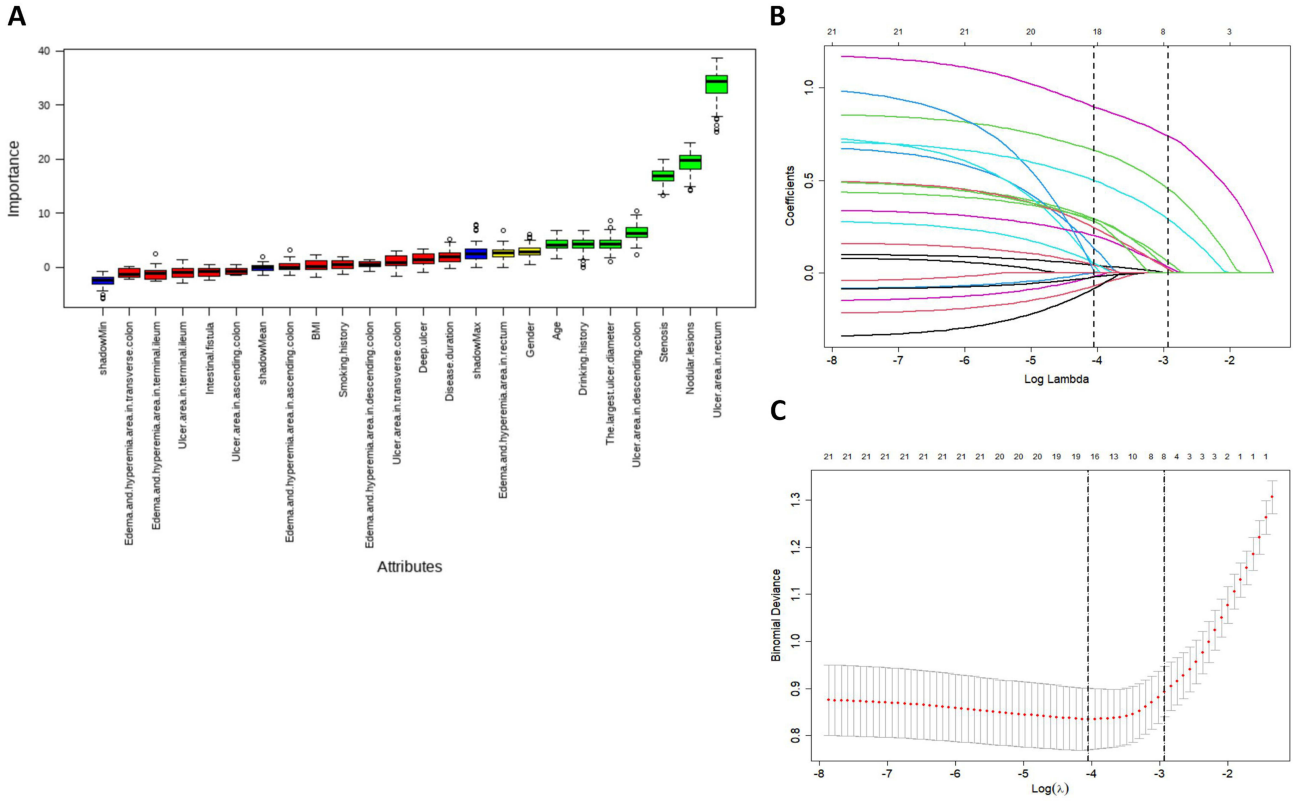

Figure 3 Feature screening via Boruta algorithm. (**A**) Feature screening via Boruta algorithm. Green bars represent confirmed significant variables (n = 7); blue bars represent shadow variables (shadowMin, shadowMax, shadowMean), which are internal negative controls to assess feature importance. (**B**) Selection of the bias-adjusted parameter (λ) in LASSO regression, with x-axis labeled as Log(λ). (**C**) Coefficient profile plot based on the log(λ) sequence. Features were selected according to the 1-SE rule (n = 8), with x-axis labeled as Log(λ).

https://doi.org/10.2147/JIR.S594754

Model Establishment

The 5 features from the intersection were included in multivariate logistic regression to develop the predictive model (Figure 4). The resulting model equation is as follows:

Logit(P(PPC)) = −5.579 + 0.408 × (largest ulcer diameter, cm) + 1.065 × (rectal ulcer area, ordinal category) + 0.338 × (descending colon ulcer area, ordinal category) + 0.681 × (nodular lesions, ordinal category) + 0.933 × (stenosis, ordinal category).

Model Performance Evaluation

ROC curves, calibration curves, DCA, and nomogram score distribution were employed to appraise model performance. In the training set, the model achieved an AUC of 0.892 (95% CI: 0.855–0.928), with a sensitivity of 0.720 and specificity of 0.902. The internal validation set showed an AUC of 0.857 (95% CI: 0.794–0.921), sensitivity of 0.795, and specificity of 0.809. The external validation set had an AUC of 0.847 (95% CI: 0.775–0.919), sensitivity of 0.700, and specificity of 0.851 (Figure 5A–C). The slight decrease in AUC is an expected and clinically acceptable finding, suggesting that there may be no obvious overfitting and supporting the model's good generalizability. Good calibration was observed across all sets, with Hosmer–Lemeshow test P-values of 0.836, 0.240, and 0.498 and calibration slopes of 1.000, 0.843, and 0.845 for the training, internal validation, and external validation sets, respectively, indicating that the model had well goodness of fit (Figure 5D–F). The model yielded positive net benefits when threshold probabilities ranged from 0.01–0.90, 0.01–0.85, and 0.05–0.78 for the three sets (Figure 6A–C). There is a significant difference in nomogram score distribution between PPC and non-PPC groups (P<0.01), confirming good diagnostic performance (Figure 6D–F).

To ease intuitive interpretation, a nomogram was constructed and proved with a clinical case (Figure 7A and B). For clinical utility, an online calculator is freely accessible at https://zsy2001.shinyapps.io/DynNomapp/.

This study makes an incremental contribution to CD PPC risk prediction. Our work formalizes these routinely collected ileocolonoscopic features into a quantitative, easy-to-use nomogram with validated performance across two independent clinical centers. The model's discriminative performance (AUC 0.847–0.892) is consistent with that of other well-validated clinical prediction models for IBD-related complications reported in the literature.[18]

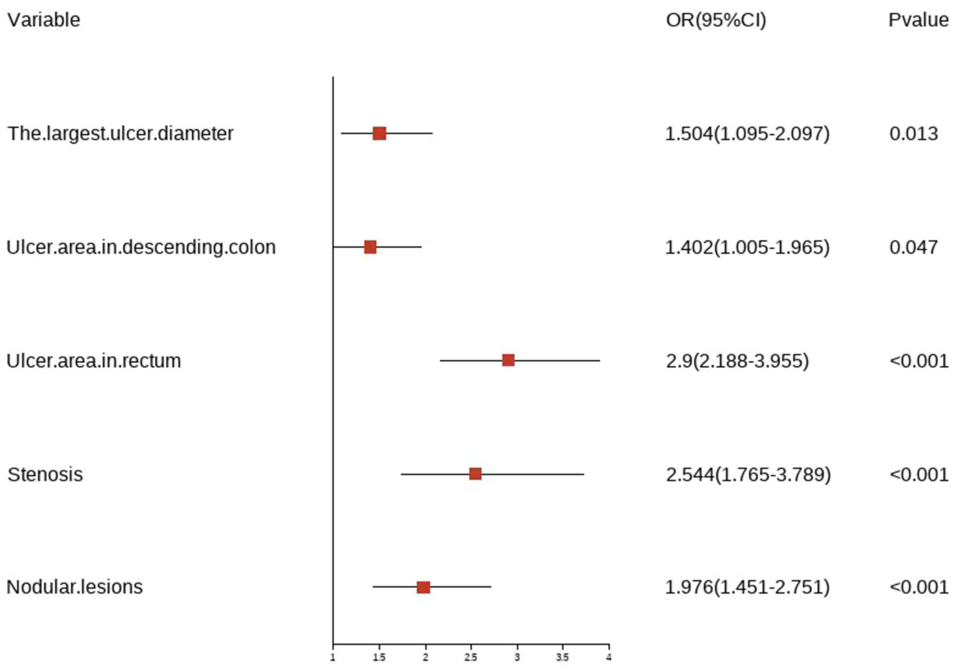

Figure 4 Forest plot of multivariate logistic regression analysis. The horizontal lines are 95% confidence intervals (CIs), and the red squares denote the odds ratios (ORs). The vertical dashed line shows the null effect (OR=1). Variables with 95% CIs that do not cross the null line are considered statistically significant (P<0.05).

https://doi.org/10.2147/JIR.S594754

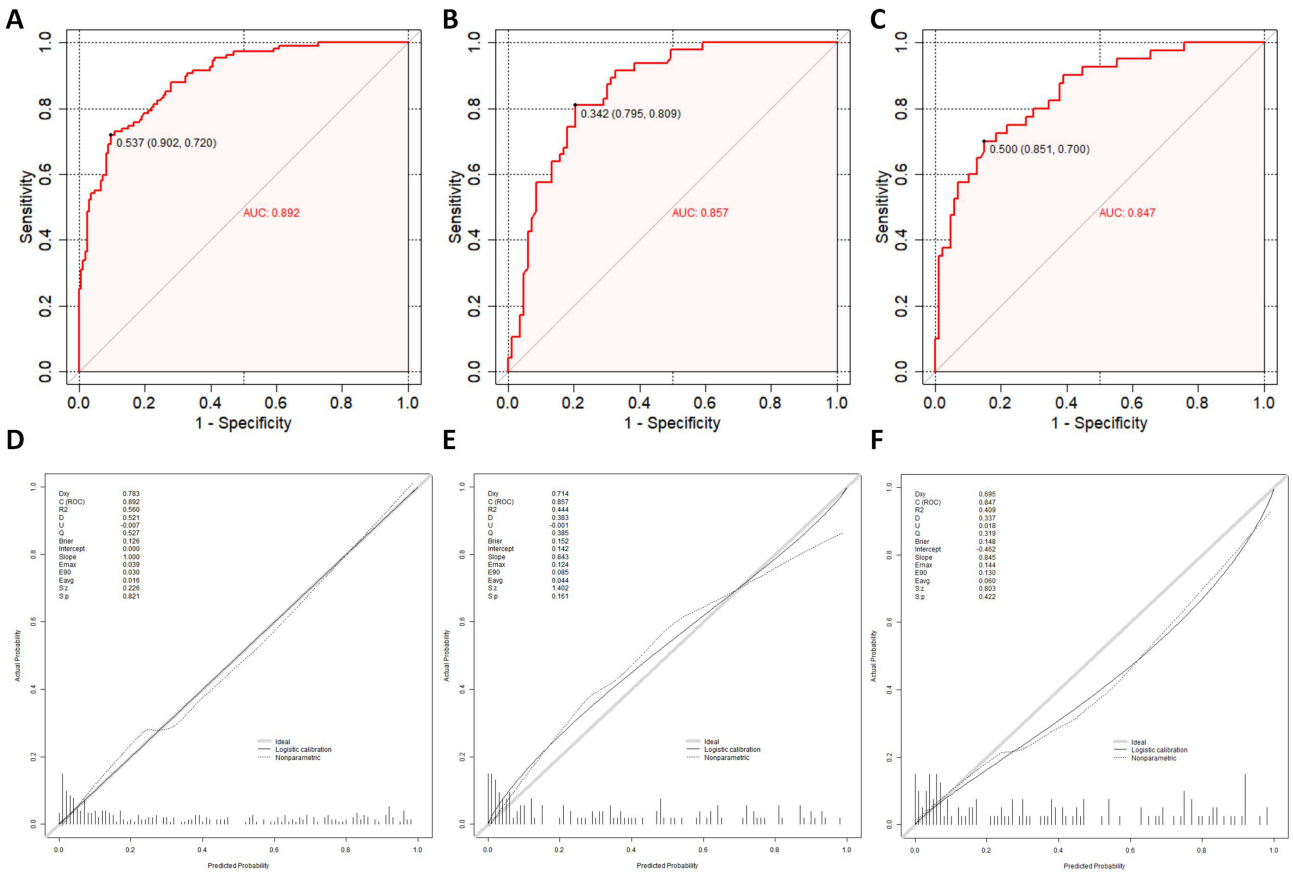

Figure 5 ROC curves and calibration curves. (**A**) Training set: AUC = 0.892 (95% CI: 0.855–0.928), sensitivity = 0.720, specificity = 0.902. (**B**) Internal validation set: AUC = 0.857 (95% CI: 0.794–0.921), sensitivity = 0.795, specificity = 0.809. (**C**) External validation set: AUC = 0.847 (95% CI: 0.775–0.919), sensitivity = 0.700, specificity = 0.851. (**D**), (**E** and **F**) are calibration curves for the three sets. Hosmer–Lemeshow and Spiegelhalter Z-tests, P > 0.05.

Discussion

We identified the largest ulcer diameter, ulcer area in rectum, ulcer area in descending colon, nodular lesions and stenosis as predictors of PPC in CD patients and constructed a risk prediction model accordingly. All of predictors were derived from observations of effectively explored intestinal segments, cutting the need for complex calculations and assumption of indetectable segments. Our study shows that features extracted from ileocolonoscopy can effectively predict PPC occurrence with high discrimination ability.

Both SES-CD and CDEIS include ulcers as reliable scoring items. Ma et al[19] developed EASE-CD—a continuous CD activity measurement tool based on ulcer diameter and area ratio with promising performance. Pathogenetically, both ulcers and PPC stem from transmural inflammation. TNF-α, IL-6, IL-1βinduces macrophages, neutrophils, and fibroblasts to secrete MMPs, damaging the mucosal basement membrane and driving ulcer progression to the submucosa, muscularis, and serosa.[20] In the perianal region, the cytokine-induced EMT is critical for fistula and abscess formation. EMT-transformed intestinal epithelial cells invade deep tissues, form tubular structures, and connect to other organs or the body surface.[21] Additionally, dysbiosis may also contribute to fistula formation.[22] Jain et al[23] found that *Debaryomyces hansenii* is enriched in the intestinal tissues of CD, potentially impairing mucosal healing; this dysregulated tissue repair capacity may contribute to the pathogenesis of PPC.[24] Our study showed the largest ulcer diameter, ulcer area in rectum and descending colon as independent risk factors for PPC.

Colonic and rectal involvement has been identified as risk factors for PPC,[25,26] while ileal involvement and isolated small intestinal lesions exert a protective effect.[27] This association is attributable to anatomical features: first, the colorectum is closer to the perianal region than the proximal intestine, rendering it more susceptible to inflammatory invasion; second, the loose areolar spaces, sphincter complexes, and glandular tissues around the distal rectum and anal

https://doi.org/10.2147/JIR.S594754

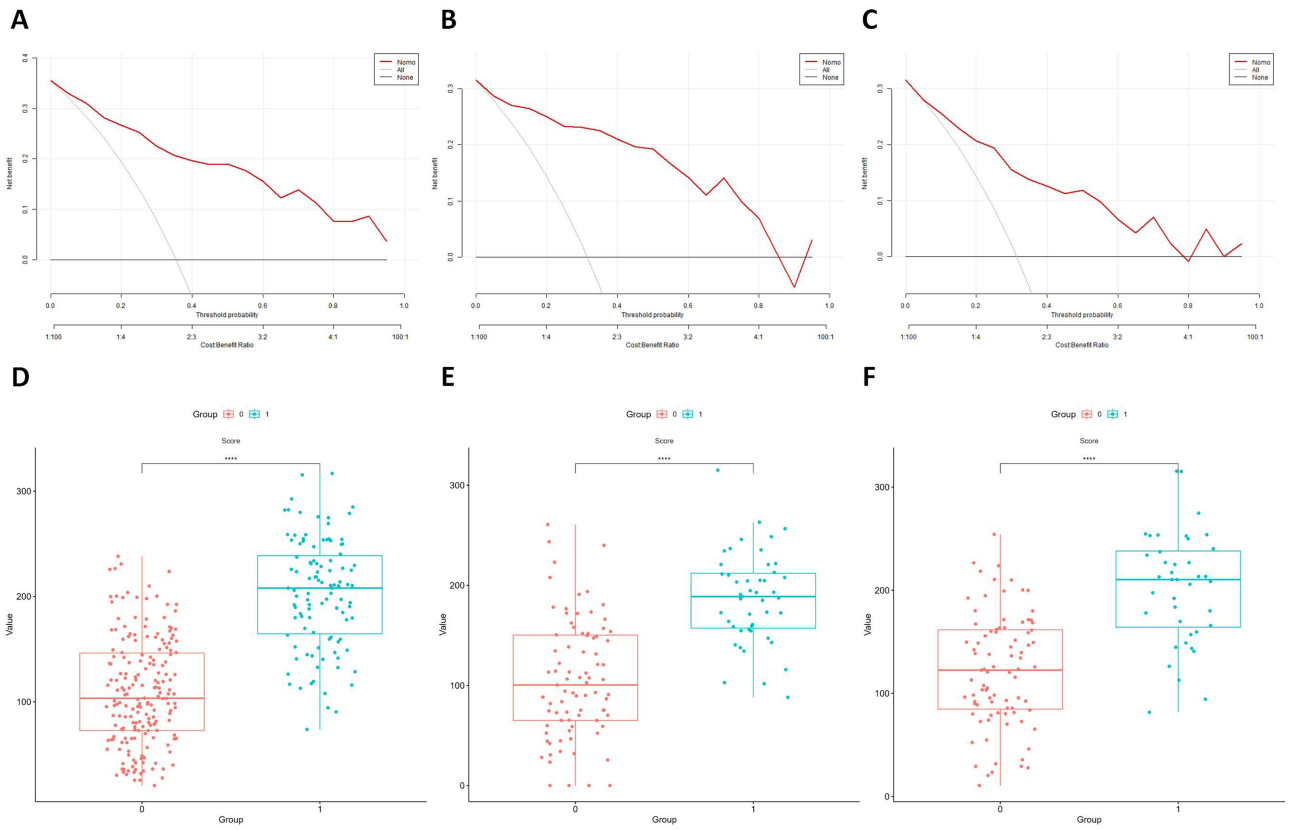

Figure 6 DCA and nomogram score distribution boxplots. (**A** and **B**) and (**C**) are DCA of model in 3 sets, respectively. x-axis = threshold probability, y-axis = net benefit. Red line = model-identified CD patients with PPC; All/None lines = extreme strategies of all/none CD patients with PPC. Positive net benefits across thresholds (0.01–0.90, 0.01–0.85, 0.05–0.78) confirm good clinical utility. (**D**–**F**) are nomogram score distribution boxplots in 3 sets, respectively. Pink dots = CD patients without PPC; cyan dots = CD patients with PPC. Boxes = 75th percentile (top), median (middle), 25th percentile (bottom). Four asterisks above 2 boxes = significant between-group distribution difference ($P < 0.05$).

canal may accelerate the formation of transmural penetration. Notably, SES-CD and CDEIS assign equal weight to lesions regardless of intestinal segments or types.[12] Our study addressed this limitation and confirmed that ulcer in the rectum and descending colon—not edema and hyperemia, or ulcers in other segments—increase PPC risk, with the risk escalating as the ulcer area ratio expands.

Besides ulcers, stenosis is incorporated as items in scoring systems yet conflicting findings exist on the stenosis-PPC association. The Korean CONNECT study did not find substantive discrepancy in PPC prevalence between participants with and without stenosis,[28] while the Japanese iCREST-CD study linked stenosis to a lower incidence of PPC.[29] However, U.S. and French studies reported opposite results.[27,30] Despite sharing an inflammatory basis, PPC and stenosis differ in cellular composition: TGF-β-regulated myofibroblasts drive stricturing fibrosis,[31,32] whereas M1 macrophages and Th17/Th1/Th17/1 T cells predominate in fistula linings and adjacent tissues.[21,33] However, EMT may also mediate stenosis formation, as TGF-β triggers intestinal epithelial EMT to upregulate ECM-related protein expression,[34] and EMT inhibition preserves intestinal epithelial features.[35] Our study confirmed stenosis as a PPC risk factor and further clarified the risk contribution of different stenosis severities.

Nodular lesions are a characteristic endoscopic feature of CD yet absent from existing scoring systems, while the cobblestone sign is one of its preliminary diagnostic criteria.[4,36] Their formation relies on mucosal hyperplasia and ulcer distribution: residual mucosal islands between CD intestinal ulcers protrude under inflammatory stimulation, contrasting with adjacent ulcer defects to form visible nodular lesions; clustered continuous ulcers make these nodules endoscopically identifiable as the cobblestone sign.[36] No direct link between nodular lesions and perianal disease has been found, but such lesions show progressive intestinal inflammation—from initial transmural inflammation to mucosal hyperplasia and thickening induced by chronic inflammation, and finally to ulcer margin consolidation via fibrotic repair.[31,37] We

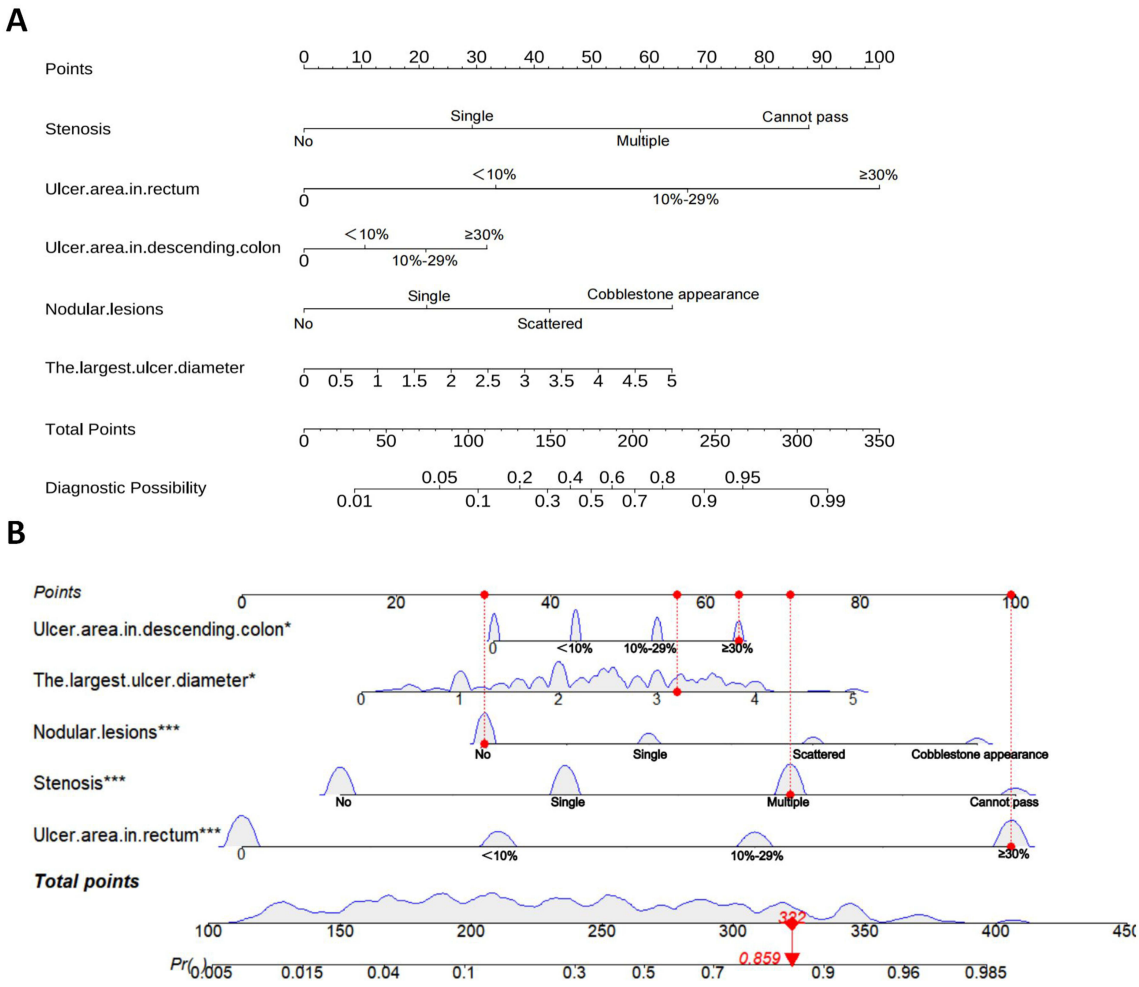

Figure 7 Static-dynamic nomogram. (**A**) Static nomogram for predicting the risk of PPC in CD patients. (**B**) Dynamic nomogram for predicting the risk of PPC in CD patients. * denotes P < 0.05, indicating the predictor has a statistically significant association with PPC occurrence; *** denotes P < 0.001, indicating the predictor has an extremely statistically significant association with PPC occurrence.

tentatively included this characteristic and confirmed that it is a risk factor for PPC. Further validation in larger, diverse populations is warranted, given this study's retrospective two-center design.

Besides the disease behavior discussed above, B3 (penetrating lesions such as intestinal fistula or intra-abdominal abscesses) and p (perianal disease such as fistula or abscess) are key Montreal classifications in CD and closely associated with PPC development. Patients with baseline p phenotype were excluded at recruitment, eliminating their confounding effect upfront. Intestinal fistula was included as an endoscopic variable but not retained by LASSO and Boruta feature selection. Nevertheless, intestinal fistula and other abdominal penetrating lesions may still confound PPC occurrence, given shared pathophysiological mechanisms including transmural inflammation, EMT, and anatomical proximity.[38]

Biologics, immunomodulators, 5-ASA agents, and glucocorticoids are core treatments for CD that suppress transmural inflammation and reduce complications including PPC. Infliximab is recommended as first-line therapy for PPC remission.[4] A recent UK PROFILE trial demonstrated that early infliximab plus immunomodulator significantly reduces fistulas, strictures, and surgeries.[39] Thus, medication exposure represents an important potential confounder for PPC risk prediction. In this study, baseline medications were fully reported. Exclusion of medication data from analysis was based on rigorous methodological and clinical considerations. As a long-term retrospective study, medication regimens varied substantially according to disease activity and treatment response. Heterogeneity was further increased by the 2023 inclusion of infliximab in the Chinese national reimbursement drug list, which altered access, adherence, and

https://doi.org/10.2147/JIR.S594754

maintenance therapy. Static baseline data cannot reflect dynamic treatment changes or poor adherence, potentially introducing bias and reducing model stability. Our primary aim was to develop a practical prediction tool using routine, objective, and readily available ileocolonoscopic features for real-time point-of-care risk stratification.

Clinical Translation and Real-World Implementation

This nomogram is designed to complement clinical risk stratification for PPC in CD. Our nomogram offers clinical value in following scenarios: pre-emptive risk stratification for asymptomatic patients, for those with high nomogram scores but no overt PPC, the model supports early treatment escalation before irreversible disease develops; risk refinement for intermediate-risk patients, it can further stratify patients with moderate endoscopic activity into high- and low-risk subgroups to guide personalized management; and integration with multi-modal assessment, it can be combined with conventional risk factors and pelvic MRI to enhance comprehensive risk stratification.

Limitation

First, although multivariable logistic regression was selected for its high clinical interpretability and suitability for nomogram construction, this approach cannot accommodate censored data or variable follow-up durations, which may introduce classification bias. Second, the required sample size was calculated as 646–793 based on a Cox–Snell R^2 of 0.25, so the model carries a potential risk of overfitting. However, the EPV ratio (19.4; 194 events, 5 predictors) exceeded the recommended threshold of 10, supporting adequate sample size. Multiple strategies, including 10-fold cross-validation in LASSO selection and internal/external validation, were used to minimize overfitting. Third, baseline and follow-up medications were not included in the model; however, we reported baseline medications, evaluated their confounding effects, and justified exclusion of these variables. Fourth, we considered the potential confounding effect of Montreal B3 phenotype. Fifth, this single-country study may have limited generalizability to other populations and settings, requiring further external validation. Other limitations include potential selection bias, incomplete visualization of the proximal small bowel, operator-dependent measurement variability, and restricted applicability in patient's ineligible for ileocolonoscopy. Future studies will integrate multi-modal data to improve model performance and clinical utility.

Conclusions

This study identified several ileocolonoscopic features associated with PPC in CD and developed a corresponding nomogram. The nomogram showed favorable discrimination, calibration, and clinical utility in two Chinese tertiary hospitals. Consistent with ECCO initiatives, this work facilitates early complication surveillance and personalized management of CD. High-risk patients may benefit from intensified monitoring and early aggressive anti-inflammatory therapy, though prospective trials are needed to validate such preventive strategies. Future studies will evaluate its performance in predicting treatment response, surgical outcomes, and severe disease courses. Further external validation in geographically and ethnically diverse cohorts, as well as integration with cross-sectional imaging and biomarker-based models, is required to confirm its generalizability.

Abbreviations

CD, Crohn's disease; PPC, Perianal penetrating complications; FAHAUTCM, First Affiliated Hospital of Anhui University of Chinese Medicine; ABSHASUTCM, Anhui Branch of Shuguang Hospital Affiliated to Shanghai University of Chinese Medicine; LASSO, Least Absolute Shrinkage and Selection Operator; ROC, Receiver Operating Characteristic; AUC, Area Under the ROC Curve; DCA, Decision Curve Analysis; ECCO, European Crohn's and Colitis Organization; SES-CD, Simple Endoscopic Score for CD; CDEIS, CD Endoscopic Index of Severity; BMI, Body Mass Index; IQR, Interquartile Range; SD, Standard Deviation; PEG-ELS, Polyethylene glycol and electrolyte oral solution; OR, Odds Ratios; CI, Confidence Intervals; TRIPOD, Transparent Reporting of a multivariable prediction model for Individual Prognosis or Diagnosis; VIF, Variance Inflation Factor.

Data Sharing Statement

The data supporting the findings of our study are available from the first author upon reasonable request.

Ethical Statement

Our study was approved by the Ethics Committees of the First Affiliated Hospital of Anhui University of Chinese Medicine (No. 2025AH-188) and Shuguang Hospital Affiliated to Shanghai University of Chinese Medicine, Anhui Branch (No. 2025SGH-EAD-022). As a purely retrospective study analyzing anonymized medical imaging data with strict anonymization protocols, it followed Article 32 of the Declaration of Helsinki for retrospective data use. Informed consent was waived by the ethics committees given no potential risks to patient welfare.

Author Contributions

Siyuan Zhang: Conceptualization, Methodology, Investigation, Data Curation, Formal Analysis, Writing - Original Draft.

Jianmin Wang: Investigation, Data Curation, Validation, Writing - Review & Editing.

Qing Lin: Resources, Data Collection, Writing - Review & Editing.

Yuqin Sheng: Resources, Data Collection, Validation, Writing – Review & Editing.

Ming Li: Conceptualization, Supervision, Funding Acquisition, Methodology, Writing - Review & Editing, Project Administration, Final Approval of Manuscript.

All authors gave final approval of the version to be published; have agreed on the journal to which the article has been submitted; and agree to be accountable for all aspects of the work.

Funding

The Natural Science Foundation of Anhui Province (No. 2408085MH227) supported our study.

Disclosure

The authors have no other conflicts of interest to declare.

References

1. El-Hussuna A, Lemser CE, Iversen AT, et al. Risk of anorectal cancer in patients with Crohn's disease and perianal fistula: a nationwide Danish cohort study. *Colorectal Dis*. 2023;25(7):1453–1459. doi:10.1111/codi.16581
2. Johansen MP, Wewer MD, Krarup PM, et al. Cancer characteristics, prognoses, and mortality of colorectal cancer in patients with Crohn's disease-a Danish nationwide cohort study, 2009-2019. *J Crohns Colitis*. 2025;19(3):jjae153. doi:10.1093/ecco-jcc/jjae153
3. Song EM, Lee HS, Kim YJ, et al. Incidence and outcomes of perianal disease in an Asian population with Crohn's disease: a nationwide population-based study. *Dig Dis Sci*. 2020;65(4):1189–1196. doi:10.1007/s10620-019-05819-9
4. Kucharzik T, Taylor S, Allocca M, et al. ECCO-ESGAR-ESP-IBUS guideline on diagnostics and monitoring of patients with inflammatory bowel disease: part 1. *J Crohns Colitis*. 2025;19(7):jjaf106. doi:10.1093/ecco-jcc/jjaf106
5. Fumery M, Savoye G, Sarter H, et al. Long-term outcome of colonic and ileal Crohn's disease: a two-decade population-based study in pediatric-onset disease. *Inflamm Bowel Dis*. 2025;31(11):3093–3102. doi:10.1093/ibd/izaf133
6. Wang Y, Wu X, Gao W, et al. Development and validation of a novel model based on clinical characteristics to predict natural disease course progression in patients with stricturing Crohn's disease. *Therap Adv Gastroenterol*. 2025;18:17562848251358705. doi:10.1177/17562848251358705
7. Zhang B, Gao Y, Tong L, et al. Development and validation of a CTE-based radiomics nomogram for predicting clinical adverse outcomes in patients with stricturing Crohn's disease. *J Inflamm Res*. 2025;18:10681–10694. doi:10.2147/jir.S526700
8. Narula N, Wong ECL, Dulai PS, et al. Defining endoscopic remission in Crohn's disease: MM-SES-CD and SES-CD thresholds associated with low risk of disease progression. *Clin Gastroenterol Hepatol*. 2024;22(8):1687–1696.e6. doi:10.1016/j.cgh.2024.02.009
9. Yzet C, Brazier F, Derval E, et al. Impact of complete vs partial endoscopic healing on long-term outcomes in Crohn's disease: a prospective multicenter study. *J Crohns Colitis*. 2025;19(7):jjaf104. doi:10.1093/ecco-jcc/jjaf104
10. Huan PW, Mehta A, Wong ECL, et al. A review of the modified multiplier of simple endoscopic score for Crohn's disease and how to use it in clinical trials and practice. *Am J Gastroenterol*. 2025;120(10):2242–2250. doi:10.14309/ajg.0000000000003373
11. Collins GS, Reitsma JB, Altman DG, et al. Transparent reporting of a multivariable prediction model for individual prognosis or diagnosis (TRIPOD): the TRIPOD statement. *BMJ*. 2015;350:g7594. doi:10.1136/bmj.g7594
12. Daperno M, D'Haens G, Van Assche G, et al. Development and validation of a new, simplified endoscopic activity score for Crohn's disease: the SES-CD. *Gastrointest Endosc*. 2004;60(4):505–512. doi:10.1016/s0016-5107(04)01878-4
13. Riley RD, Ensor J, Snell KIE, et al. Calculating the sample size required for developing a clinical prediction model. *BMJ*. 2020;368:m441. doi:10.1136/bmj.m441
14. Hsu YC, Wu TC, Lo YC, et al. Gastrointestinal complications and extraintestinal manifestations of inflammatory bowel disease in Taiwan: a population-based study. *J Chin Med Assoc*. 2017;80(2):56–62. doi:10.1016/j.jcma.2016.08.009

15. McKay C, Bolzani A, Kienzle S, et al. Epidemiology, treatment patterns, and associated risk factors in perianal fistulizing Crohn's disease: a systematic literature review. *World J Gastrointest Surg*. 2025;17(7):101767. doi:10.4240/wjgs.v17.i7.101767
16. Colorectal Group, Chinese Society of Digestive Endoscopy. Consensus on bowel preparation for colonoscopy (2023, Guangzhou). *Chin J Digest Endosc*. 2023;40(6):421–430. doi:10.3760/cma.j.cn321463-20230607-00230
17. Peduzzi P, Concato J, Kemper E, et al. A simulation study of the number of events per variable in logistic regression analysis. *J Clin Epidemiol*. 1996;49(12):1373–1379. doi:10.1016/s0895-4356(96)00236-3
18. Yu L, Cai Y, Lin S, et al. Quantitative MRI radiomics approach for evaluating muscular alteration in Crohn disease: development of a machine learning-nomogram composite diagnostic tool. *Abdom Radiol*. 2025;50(11):5069–5078. doi:10.1007/s00261-025-04896-x
19. Ma C, Khanna R, Maguire BR, et al. Development and validation of a novel endoscopic ulcer activity score for evaluation of Crohn's disease (EASE-CD) using data from two randomised controlled trials. *Lancet Gastroenterol Hepatol*. 2025;10(8):746–756. doi:10.1016/s2468-1253(25)00093-7
20. Maronek M, Marafini I, Gardlik R, et al. Metalloproteinases in inflammatory bowel diseases. *J Inflamm Res*. 2021;14:1029–1041. doi:10.2147/jir.S288280
21. Rizzo G, Rubbino F, Elangovan S, et al. Dysfunctional extracellular matrix remodeling supports perianal fistulizing Crohn's disease by a mechanoregulated activation of the epithelial-to-mesenchymal transition. *Cell Mol Gastroenterol Hepatol*. 2023;15(3):741–764. doi:10.1016/j.jcmgh.2022.12.006
22. Breton J, Tanes C, Tu V, et al. A Microbial signature for paediatric perianal Crohn's disease. *J Crohns Colitis*. 2022;16(8):1281–1292. doi:10.1093/ecco-jcc/jjac032
23. Jain U, Ver Heul AM, Xiong S, et al. Debaryomyces is enriched in Crohn's disease intestinal tissue and impairs healing in mice. *Science*. 2021;371(6534):1154–1159. doi:10.1126/science.abd0919
24. McGregor CGC, Tandon R, Simmons A. Pathogenesis of fistulating Crohn's disease: a review. *Cell Mol Gastroenterol Hepatol*. 2023;15(1):1–11. doi:10.1016/j.jcmgh.2022.09.011
25. Brochard C, Rabilloud ML, Hamonic S, et al. Natural history of perianal Crohn's disease: long-term follow-up of a population-based cohort. *Clin Gastroenterol Hepatol*. 2022;20(2):e102–e110. doi:10.1016/j.cgh.2020.12.024
26. Martinez Sanchez ER, Sola Fernandez A, Perez Palacios D, et al. Perianal Crohn's disease: clinical implications, prognosis and use of resources. *Rev Esp Enferm Dig*. 2022;114(5):254–258. doi:10.17235/reed.2021.7918/2021
27. Kaur M, Panikkath D, Yan X, et al. Perianal Crohn's disease is associated with distal colonic disease, stricturing disease behavior, IBD-associated serologies and genetic variation in the jak-stat pathway. *Inflamm Bowel Dis*. 2016;22(4):862–869. doi:10.1097/mib.0000000000000705
28. Chun J, Lm JP, Kim JW, et al. Association of perianal fistulas with clinical features and prognosis of Crohn's disease in Korea: results from the CONNECT study. *Gut Liver*. 2018;12(5):544–554. doi:10.5009/gnl18157
29. Yamamoto T, Nakase H, Watanabe K, et al. Diagnosis and clinical features of perianal lesions in newly diagnosed Crohn's disease: subgroup analysis from Inception Cohort Registry Study of Patients with Crohn's Disease (iCREST-CD). *J Crohns Colitis*. 2023;17(8):1193–1206. doi:10.1093/ecco-jcc/jjad038
30. Danielou M, Sarter H, Pariente B, et al. Natural history of perianal fistulising lesions in patients with elderly- onset Crohn's disease: a population-based study. *J Crohns Colitis*. 2020;14(4):501–507. doi:10.1093/ecco-jcc/jjz173
31. Bauer-Rowe KE, Pham B, Griffin M, et al. Creeping fat-derived mechanosensitive fibroblasts drive intestinal fibrosis in Crohn's disease strictures. *Cell*. 2025;188(23):6536–6553.e26. doi:10.1016/j.cell.2025.08.029
32. Ito T, Kayama H. Roles of fibroblasts in the pathogenesis of inflammatory bowel diseases and IBD-associated fibrosis. *Int Immunol*. 2025;37(7):377–392. doi:10.1093/intimm/dxaf015
33. Lightner AL, Ashburn JH, Brar MS, et al. Fistulizing Crohn's disease. *Curr Probl Surg*. 2020;57(11):100808. doi:10.1016/j.cpsurg.2020.100808
34. Macias-Ceja DC, Mendoza-Ballesteros MT, Ortega-Albiach M, et al. Role of the epithelial barrier in intestinal fibrosis associated with inflammatory bowel disease: relevance of the epithelial-to mesenchymal transition. *Front Cell Dev Biol*. 2023;11:1258843. doi:10.3389/fcell.2023.1258843
35. Gao Y, Lu LJ, Zhang ZZ, et al. Xue-Jie-San prevents the early development of colitis-associated intestinal fibrosis by blocking Notch1 and FGL1 signaling pathways. *J Ethnopharmacol*. 2023;315:116678. doi:10.1016/j.jep.2023.116678
36. Kochhar GS, Dziegielewski C, Schairer JN, et al. Role of endoscopy in inflammatory bowel disease: what every gastroenterologist should know. *Am J Gastroenterol*. 2025;120(11):2502–2509. doi:10.14309/ajg.0000000000003507
37. Rieder F, Mukherjee PK, Massey WJ, et al. Fibrosis in IBD: from pathogenesis to therapeutic targets. *Gut*. 2024;73(5):854–866. doi:10.1136/gutjnl-2023-329963
38. Basiji K, Kazemifard N, Farmani M, et al. Fistula in Crohn's disease: classification, pathogenesis, and treatment options. *Tissue Barriers*. 2025;13(3):2458784. doi:10.1080/21688370.2025.2458784
39. Noor NM, Lee JC, Bond S, et al. A biomarker-stratified comparison of top-down versus accelerated step-up treatment strategies for patients with newly diagnosed Crohn's disease (PROFILE): a multicentre, open-label randomised controlled trial. *Lancet Gastroenterol Hepatol*. 2024;9(5):415–427. doi:10.1016/s2468-1253(24)00034-7